Mon. Not. R. Astron. Soc. **000**, 000–000 (0000) Printed 24 April 2013 (MN LATEX style file v2.2)

The baryonic properties of the Local Group in a cosmological context: a semi-analytic perspective

Sergio Sanes ⋆[1], Jaime E. Forero-Romero[2], Juan C. Munoz-Cuartas[1], Luis F. Quiroga-Pelaez[1], Jorge I. Zuluaga[1], Stefan Gottlöber[3], Yehuda Hoffman[4], Gustavo Yepes[5]

[1] *Instituto de Física - FCEN, Universidad de Antioquia, Calle 67 No. 53-108, Medellín, Colombia*
[2] *Departamento de Física, Universidad de los Andes, Cra. 1 No. 18A-10, Edificio Ip, Bogotá, Colombia*
[3] *Leibniz-Institut für Astrophysik Potsdam (AIP), An der Sternwarte 16, 14482 Potsdam, Germany*
[4] *Racah Institute of Physics, Hebrew University, Jerusalem 91904, Israel*
[5] *Grupo de Astrofísica, Universidad Autónoma de Madrid, Madrid E-28049, Spain*

24 April 2013

ABSTRACT

We present a series of models that follow the evoluciont of the two dominant galaxies in the Local Group: the Milky Way (MW) and M31. We use semi-analytic techniques coupled to three N-body constrained cosmological simulations. Each simulated volume contains a pair of halos with environmental conditions similar to the observed for the LG. The models are computed using the public available code Galacticus. The main objective is to study the conditions to get the best possible agreement in three barionic properties for the MW and M31: the stellar mass, gaseous mass and disc-to-bulge mass ratio. Each physical model varies the parameters controlling the star formation efficiency and supernovae feedback. The models are run on a general sample of dark halos with a mass range of $7 \times 10^{11} h^{-1}\mathrm{M}_{\odot} < M_{\mathrm{h}} < 7 \times 10^{12} h^{-1}\mathrm{M}_{\odot}$. For the model that best reproduce the global properties of galaxies in this halo mass range, we find that the most probable values for the baryonic properties are $M_{\star} =$, $M_{\mathrm{gas}} =$ and $f_{D/B} =$. The three LG in the constrained simulation have values $M_{\star} =$, $M_{\mathrm{gas}} =$ and $f_{D/B} =$.

Key words: galaxies: evolution - galaxies: formation - galaxies: high-redshift - methods: N-body simulations

1 INTRODUCTION

Some of the most challenging problems of studying galaxy formation are our distance limitation to acquire data from galaxies or even bigger structures and the time scale of the physical processes involved, so, the best laboratories we can find are the closest ones. The Local Group galaxies (LG), particulary the Milky Way (MW) and M31 are the ones from where we can get more detailed observations. Because of the latter, ongoing and new surveys like the Sloan Digital Sky Survey (Abazajian et al. 2009), the Large Synoptic Survey Telescope (LSST) (LSST Science Collaboration et al. 2009), VLT Survey Telectope (Capaccioli & Schipani 2011) are dedicating efforts in providing crucial information to encrease our comprehension on the kinematics, structure, formation and evolution of our galaxy. Nevertheless, our understanding of galaxy formation would never be complete without studying a high quantity of galaxies. Over the past two decades the amount of observations from surveys providing extragalactic data like the SDSS,..EXAMPLES..., has increased dramatically. Evenmore, the amount of data will exponentially grow even faster with projects like LAMOST (Newberg et al. 2009), LSST and SkyMapper (Keller et al. 2007). But, despite of the currrent and upcomming data, there are no analytical models able to properlly interpret these observations and with predictive capacity to accurately describe the evolution and formation of a galaxy and then clear our comprehension of the real physical phenomena involved in such process.

Another challenging problem is the large number of physical phenomena implicated in the process of galactic evolution. The large scale and composition of structures like galaxies, where baryonic matter can be found in several phases implies different physics at each scale and phase.

⋆ email

The nowadays standard description of hierarchical galaxy formation was first introduced by White & Rees (1978) and has been enhanced since then. According to it, primitive gaussian inhomogenities are amplified by gravitational instabilities producing small density fluctuations of dark matter that grow until collapses into haloes, then, baryonic matter is attracted inside the potencial well of these, producing a hot gaseous halo. With time, a fraction of gas from the hot halo is free to cool and condese forming a central disc. Inhomogenities in the central disc allow to form smaller objects with higher density like stars. The process of star formation is regulated by severalphenomena like stellar stellar, supernovae and AGN feedbacks.

The complex behaviour of the physical phenomena shown by galaxies has stated the necessity to tackle the problem of galaxy formation from different angles. Up to date, two methods have been consolidated as the cornerstones of galaxy formation: Numerical and semi-analytical simulations. The former are the most commonly used. This method can be implemented at several levels of approximation to reality: doing dissipationless N-body simulations neglecting gas dynamics; another approach is done by including a dissipational component, where, different physical processes are taken into account under certain approximations and the ones of highest complexity are the multi-physics hydrodynamical simulations where phenomena like, cooling flows, star formation, feedbacks or even more complex processes can be included in a high realistic manner.

Over the past years, codes like Gadget (Springel 2005), RAMSES (Teyssier 2002) and AREPO (Springel 2010) have proven to be valuable tools, increasing the credibility of the method. Some well known cosmological simulations are the Millenium (Springel et al. 2005), Bolshoi (Klypin et al. 2011), Aquarius (Springel et al. 2008) and CLUES (Gottloeber et al. 2010). In this paper we make use of the dark matter merger trees catalogue provided by the CLUES simulations, this are characterized for been constrained to accurately recreate the local Universse. Despite of the great successfull of this method, the large amount of computational resources that these requires, limitats its usage to the available technological infrastructure, thus, restricting the number of simulations of any research to a few ones. This disadvantage, hinders the study of large quantities models, which is necessary to provide a deep understanding in the evolution of galaxies .

On the other side are the semi-analytical simulations, which where first proposed by White & Frenk (1991) based on the ideas of hierarchical evolution. These models combine the description of the evolution of dark matter haloes from a cosmological background via dark matter halo merger trees provided either from large cosmological N-body simulations or by the Press-Schechter formalism (Press & Schechter 1974) with a phenomenological description of any astrophysical process. Using as input the information contained in the merger histories, these models can follow the evolution of the baryonic matter starting at high redshift to any stage. Considering the formation of a hot haloe, a cooling process and the condesation of cold gas into a central disc through apparently simple recipes, any of the componing phases of a galaxy (hot halo, cold disc, stars and ejecta) can be estimated. To regulate the star formation it is tipically introduced stellar and supernovae feedback, and more recently for high mass galaxies, AGN feedback was added to reproduce the luminosity function at the bright end (Croton et al. 2006). Central bulges and bars are generated by the occurrence of mergers between central and satellites galaxies. There is a large amount of physical phenomena that can be included in these models. In general all the astrophysical processes included in any semi-analytical model are dependent on a number of free parameters that are usually contrained from observations.

The greatest advantage of semi-analytitical models is its computational versatility. These simulations are very fast and low cost, thus, can be implemented as many times as necessary. Besides, currently have great successfull in reproducing global properties of galaxies. Over the last years, the interest of these simulations has increased. Some renamed codes are Galacticus (Benson 2010), GALFORM (Benson & Bower 2010) and ChemTree (Tumlinson 2006) among others. Notwithstanding the capabilities of the semi-analitycal simulations, these are intended to statistically reproduce the properties of the galaxies ,and then, are in general limited to only estimate external properties and morphology of them i.e like the radius and mass of the componing phases of the bulge or disc.

We use the code Galacticus[1] to study from a semi-analitycal view the problem of galaxy formation in the neighboring Universe. A key feature of our research is the usage of merger trees provided by CLUES. Maybe the most important aspect of these, are their hability to produce a set of dark matter halos that mimics the characteristics of the Local Group , thus, recreating the hosting haloes the MW, M31 and M33, wich we call the 'LG candidates'. Exploding the advantages of contrained simulations, we aim investigate the space parameter of the set of physical processes that drives the formation and morphology of galaxies in the Local Universe, how does these affect the statistical properties of this population and whether they modify the abundace of MW and M31-like galaxies or not. We also give special attention to the MW and M31 candidates and study the similarities of the mock galaxies to the observed ones.

This paper is organized as follows. In section 2 we present the information regarding the data we use as input and the main features of the theoretical models implemented in the semi-analitycal code. In section 3 is summarized the current observational data of the Local Group we use to compare our results. In section 4 is described how we proceed to reach our goals. In section 5 we present the results and discuss about them. Finally, in section 6 we summarize our results and present the conclusions of this work.

2 NUMERICAL METHODS

2.1 Contrained N-body simulations and Merger Trees

In this section we briefly describe the details of the CLUES[2] project[3] relevant to our research, the procedure of constraining cosmological simulations and construction of merger

[1] `https://sites.google.com/site/galacticusmodel/about`
[2] Constrained Local UniversE Simulations
[3] `http://www.clues-project.org/`

trees. We have selected the three available realizations for the WMAP5 cosmology of CLUES, which is aimed to provide constrained cosmological simulations recreating the Local Universe. Each of these simulations includes 1024^3 particles with a mass of $m_p = 1.89 \times 10^7 h^{-1}\mathrm{M}_\odot$inside a box of length $64h^{-1}$Mpc that provides an amount of more than 5×10^4 dark matter merger trees. The cosmological parameters are consistent with the WMAP5 cosmology in Komatsu et al. (2009) with a density $\Omega_m = 0.279$, a cosmological constant $\Omega_\Lambda = 0.721$, a dimensionless Hubble parameter $h = 0.70$, a spectral index of primordial density perturbations $n = 0.96$, a normalization $\sigma_8 = 0.817$.

The code used to perform the simulations is the Tree-PM MPI N-body code Gadget2 (Springel 2005). We selected the set of merger trees whose dark matter halos at $z = 0$ are in the mass range $11.0 < \log_{10} M_{vir}/M_\odot < 13.0$ and made emphasis in the subrange $11.5 < \log_{10} M_{vir}/M_\odot < 12.5$ to study MW and M31-type galaxies. As mentioned above, we will give special attention to those "candidates" halos supposed to host a MW and M31. The amount of halos in our selected mass range is above 9000/box, thus, accounting for a total of almost 30000 merger trees when the three boxes are included.

The standard procedure of building by means of simulations a Local Universe able to recreate the main features of the observed, is to constrain the initial conditions to observations. To prepare the initial conditions of CLUES, it was used the algorithm of Hoffman & Ribak (1991) to constrain the Gaussian random fields. Due to its very small changes in time, the velocity field plays a crucial roll in constraining the initial conditions. To set up the velocity constrains, the MARK III (Willick et al. 1997), SBF (Tonry et al. 2001) and the Karachentsev (Karachentsev et al. 2004) catalogs were used (Forero-Romero et al. 2011), for more details of the constraining procedure go to Gottloeber et al. (2010). As the constrains can only affect the large and meso scales, it was necessary to perform a large amount of low resolution simulations. Only three of all the simulations had success in recreating under a certain accuracy the properties of the dark matter distribution.

To tackle the problem of halo identification, it was used a FOF (Friends-of-Friends) algorithm through 80 snapshots corresponding to an interval of about 13Grys between $0 < z < 7$, where was not resolved substructures. It was used a linking length of $b = 0.17$ times the mean inter particle separation and the minimum resolved halo masses are of $M_{\min} = 3.78 \times 10^8 h^{-1}\mathrm{M}_\odot$. The procedure used to build the merger trees is the standard. Starting from the snapshot at $z = 0$, the particles bind to a particular halo of the catalogue are scanned in the first snapshot $z > 0$ and if there it is found any halo with more than thirteen particles then then this halo is called to be a progenitor of the former. The process is repeated over the whole catalogue at $z = 0$ and continued until the highest z. For more details about the halo identification and merger tree construction go to Forero-Romero et al. (2011).

To perform our simulations, each galaxy was modelled isolatedly and it was only used the information relating the masses of the satellites and central dark matter halos to its progenitorsover through all the different snapshots.

2.2 Semi-analytical Approach

We use the semi-analytic code of galaxy formation Galacticus (Benson 2010), designed to by means of the hierarchical merging history of dark matter haloes, estimate the properties of the galaxies hosted in it at any instant of its evolution.

The code can include any model of physical process, starting from the generation of random dark matter density distributions to calculate stellar population properties while implementing accretion of gas, cooling, stellar and supernovae feedback. Depending of the needs, it is capable of generate its own Monte Carlo merger trees or just read merger trees provided by cosmological simulations as we did, taking advantage of the CLUES data. This section is dedicated to explain how Galacticus implements the key astrophysical processes regarding our research.

Mass Accretion. Two modes of mass accretion are tipically considered, rapid increase during violent mergers and smooth accretion of matter from the interstellar medium. In our theoretical model, is assumed that the amount of baryonic matter gained during the accretion of dark matter in any of the modes is directly related by the universal baryonic fraction Ω_b/Ω_M. The change of baryonic mass $\dot{M}_{\mathrm{brn}}$ is defined as:

$$\dot{M}_{\mathrm{brn}} = \begin{cases} (\Omega_b/\Omega_M)\dot{M}_{\mathrm{halo}}, & \text{if} \quad V_{\mathrm{vir}} > V_{\mathrm{rnz}} \\ & \text{or} \quad z < z_{\mathrm{rnz}} \\ 0, \text{otherwise} \end{cases} , \qquad (1)$$

where the effects of reionization are taken into account by imposing the condition that no gas can be accreted at redshifts z higher than the one of reionization z_{rnz} or if the magnitude of the virial velocity V_{vir} is less than that of reionization V_{rnz}. In case of a merger, when the satellite-to-central mass ratio $M_{\mathrm{stl}}/M_{\mathrm{ctl}}$ is above the merger fraction F_{mgr}, thus, a major merger, then the whole mass of the satellite M_{stl} and central M_{ctl} goes to the bulge component of the central galaxy.If a minor merger occurs ($M_{\mathrm{stl}}/M_{\mathrm{ctl}} < F_{\mathrm{mgr}}$) the mass of the dic of the central galaxy is not redirected, the stellar component of the satellite goes to the bulge of the central but the gas mass $M_{\text{stl-gas}}$ content of the satellite can go to either to the disc or the bulge, we can configure this situation by setting free parameter $\vec{M}_{stl-gas}$ either to disc or bulge, telling to the code what situation must occur.

Cooling. Once the halo has collapsed and the hot gas halo formed, a fraction of the gas tend cools, this redices the presure and causes the formation of a central disc through the accretion of gas. The rate at which the gas is cooled according to White & Frenk (1991) is given by

$$\dot{M}_{cool} = 4\pi r_{\mathrm{cool}}^2 \rho(r_{\mathrm{cool}}) \dot{r}_{\mathrm{cool}} \qquad (2)$$

where $\rho(r)$ is the density profile of the hot halo and the cooling raduis r_{cool} is calculted by seeking the radius at which the time available for cooling equals the cooling time t_{cool}.

The cooled gas can be transformed into stars depending on the density of the gas during a characteristic formation timescale $\tau_\star$. This depends on the rotational velocity V_{rot} of the disc according to the dynamical time $\tau_{\mathrm{dyn}} = R_{\mathrm{vir}}/V_{\mathrm{rot}}$, where R_{vir} is the characteristic radius. It is also related to

the star formation efficiency $\epsilon_\star$, which is assumed fixed. We use the expression of star formation time scale

$$\tau_\star = \epsilon_\star^{-1}\tau_{\rm dyn}\left(\frac{V}{200{\rm km/s}}\right)^{\alpha_\star}, \quad (3)$$

which is similar to that of Baugh et al. (2005), where $\epsilon_\star$ and $\alpha_\star$ are free parameters. Finally, the star formation rate of the forming stars is defined as $\phi = M_{\rm gas}/\tau_\star$, where $M_{\rm gas}$ is the gas mass.

Stellar Mass. At early stages of star formation the gas accreted is basiclly Hydrogen. The internal processes of stars produce heavier elements and when stars ends live in the form of a supernovae these elements are expulsed to the environment enriching the medium. The process of accretion continues and as stars form, the abundace of combustible material changes. We used the simplest method to model the change of stellar mass. We relate the star formation rate ϕ to the stellar mass rate $\dot{M}_\star$ by means of a constant rate of decrease of fuel mass as

$$\dot{M}_\star = (1-R)\phi, \quad (4)$$

where R is the instantaneous recycled fraction. The rate of the metal content of the fuel changes as the star formation rate, the yield p and R according to

$$\dot{M}_{{\rm fuel},Z} = -(1-R)Z_{\rm fuel}\phi + p\phi, \quad (5)$$

while the rate of change the metal content of the stars $\dot{M}_{\star,Z}$ follows from the fuel metallicity $Z_{\rm fuel}$.

Supernovae Feedback.

The process of star formation is regulated by several phenomena. One of these is the stellar feedback, where, energy expulsed by the created stars heat the surroundings preventing a fraction of gas from cooling and forming stars (REFERENCE). When stars explode as supernovae the energy released reheats the cooled gas and decreasing the production of stars. This feedback of supernovae has proven to be the dominant process that modules star formation in low and medium mass galaxies (REFERENCE).

We model this process through a power law relation and assume it to be proportional to the rate of energy pumped in to the gas by the stellar populations. The rate of change of the mass ejected by supernovae is given by

$$\dot{M}_{\rm outflow} = \left(\frac{V_{\rm outflow}}{V}\right)^{\alpha_{\rm outflow}}\frac{\dot{E}}{E_{\rm canonical}}, \quad (6)$$

where $V_{\rm outflow}$ is the velocity of the ejected outflow mass due to supernovae, V is the characteristic velocity, $\dot{E}$ is the rate of change of the energy transmitted to the gas by stars and $E_{\rm canonical}$ is the total energy transmitted by a stellar population normalized to $1M_\odot$.

In contrast, for high mass galaxies the driving process of star formation is the feedback produced by Active Galactic Nuclei (AGN) (Croton et al. 2006). Two growing modes are tipically assumed for black holes: A rapid growing occurs during galaxy mergers, where, back holes join to produce supermassive ones; This is called the "quasar mode". The other mode of growing is motivated by the accretion of gas, the "radio mode". When the gas is attracted by the black hole, it is mechanically heated. This feedback injects low enery into the surroundings that is capable to decrease the gas cooling or even stop it (Croton et al. 2006). In this paper we focus on haloes of mass lower than $1\times10^{12}M_\odot$ and then it is not necessary to include AGN feedback to our procedures.

3 OBSERVATIONAL PRORPERTIES OF MW AND M31

In this section we present the values for the parameters we have chosen to define the MW and M31: disk stellar mass, disk gaseous mass and bulge stellar mass.

Disk stellar mass. The principal approach to estimate the stellar mass in the disk of our galaxy is dynamical modelling. The work of Klypin et al. (2002) uses a parametric model that does not distinguish between the cold (gas) component and the stars, their results for galaxy models that allow for exchange of angular momentum locate the total baryonic mass of the disk between $5-6\times10^{10}{\rm M}_\odot$for the MW and $7-9\times10{\rm M}_\odot$for M31. Later Widrow & Dubinski (2005) use N-body realizations of self-consisten, equilibrium distributions of the dark matter and stellar compoents to address the same problem. Their models fit with good match to the observational data have stellar masses of $3.3-4.5\times10^{10}{\rm M}_\odot$for the Milky Way and $7-10\times10^{10}$ for andromeda. (Geehan et al. 2006a) modeled the Andromeda strem using analytic bulge-disc-halo for M31, finding the best agreement for a disk mass of $8.4\times10^{10}{\rm M}_\odot$. In this work we take $3.3-4.5\times10^{10}{\rm M}_\odot$for the Milky Way and $7-10\times10^{10}$ for M31.

Bulge stellar mass. Klypin et al. (2002) constrain the MW bulge stellar masss $1-1.2\times10^{10}$ ${\rm M}_\odot$while for M31 $1.9-2.4\times10^{10}$, for the same galaxy (Geehan et al. 2006a) find a bulge mass of $3.3\times10^{10}{\rm M}_\odot$. The MW analytical model of model (Dehnen & Binney 1998) finds a range of different values with average $\sim0.510^{10}{\rm M}_\odot$. In this work we pick $0.5-1.2\times10^{10}{\rm M}_\odot$for the MW and $1.9-3.3\times10^{10}{\rm M}_\odot$for M31.

Disk Gaseous mass. The abundance of gas in the Milky Way has been constrained through chemical evolution models. The set of observational constraints on these models most notably include the gas and star formation rate (SFR) profiles. The relevant observational data was compiled in (Boissier & Prantzos 1999) using from the original work in Kulkarni & Heiles (1987); Dame (1993), with a values of $6.0-8.0\times10^9{\rm M}_\odot$, an update implementation of this chemical evolution model by (Yin et al. 2009a) uses the same observations. In the case of M31 the best observational constraints come from the observations by (Cram et al. 1980) with the integrated mass of neutral gas corrected by (Dame 1993), yielding a value of $5.2\times10^9{\rm M}_\odot$, there is a systematic observational uncertainty of 5% originally quoted in (Cram et al. 1980), but due to oppacity effects of the HI (Braun & Walterbos 1992) the total value of gas can increase by a 19%. Therefore we keep a value of $5.0-6.0\times10^9$ for the mass of gas in the M31 disk and $6.0-8.0\times10^9{\rm M}_\odot$for the Milky Way.

Model	$z_{reioniz}$	$M_{\rm satel.,gas} \rightarrow$	$F_{\rm mgr}$	$P(\lambda)$	μ_λ	σ_λ	$\alpha_{\rm disk,outflow}$	$\epsilon_{\rm disk,\star}$
R1	9.0	bulge	0.3	Bett 2007			2.0	0.01
R2	7.0	bulge	0.3	Lognormal	0.031	0.57	2.0	0.01
R3	7.0	disk	0.3	Lognormal	0.031	0.57	2.0	0.01
E1	7.0	disk	0.3	Lognormal	0.031	0.57	2.0	0.02
E2	7.0	disk	0.3	Lognormal	0.031	0.57	2.0	0.035
E3	7.0	disk	0.3	Lognormal	0.031	0.57	2.0	0.05
E4	7.0	disk	0.3	Lognormal	0.031	0.57	2.0	0.075
E5	7.0	disk	0.3	Lognormal	0.031	0.57	2.0	0.1
A1	7.0	disk	0.3	Lognormal	0.031	0.57	1.5	0.01
A2	7.0	disk	0.3	Lognormal	0.031	0.57	2.5	0.01
A3	7.0	disk	0.3	Lognormal	0.031	0.57	3.0	0.01
D1	7.0	disk	0.2	Lognormal	0.031	0.57	2.0	0.01
D2	7.0	disk	0.4	Lognormal	0.031	0.57	2.0	0.01
B1	7.0	bulge	0.2	Lognormal	0.031	0.57	2.0	0.01
B2	7.0	bulge	0.4	Lognormal	0.031	0.57	2.0	0.01

Table 1. Set of four experiments intended to model the galaxies hosted in halos of mass range of $11.0 < log_{10} M_{\rm DM} < 13.0$.

4 THE METHOD

4.1 Parameter Space Exploration

To achieve our goals we have used the semi-analytic code Galacticus v0.0.1 to perform semi-analytical simulations of different models to study the $z = 0$ properties of the simulated galaxies. In this part of the research we study how sensitive are the properties of the simulated galaxies to the variations of several parameters we pretent to study. To do this, we have simulated a set of models with parameters as shown Table 1. We have fixed cosmologycal parameters to the WMAP5 values to be in agreement with the input data, any other not mentioned parameters are settled to the code's default values (To see the parameters in detail and their values go to Benson (2010)). From the simulated models of Table 1 we have defined three benchmarks, the first is R1 which is performed with a spin parameter distribution according to the one in Bett et al. (2007).

For he two other simulated models R2 and R3, we have settled the distribution of the spin parameter to a Lognormal distribution with a mean $\mu_\lambda = 0.03687$ and dispersion $\sigma_\lambda = 0.2216$ according to the work of Muñoz-Cuartas et al. (2011) but in R2 the gas of satellites after a minor merger goes to the bulge of the central galaxy and in the R3 the gas goes to the disk of the central galaxy. All the remaining models are fixed to a Lognormal distribution with a mean $\mu_\lambda = 0.03687$ and dispersion $\sigma_\lambda = 0.2216$ as well.

We have developed a set of four experiments intended to study how are affected the stellar-to-dark matter ratio, gas-to-total mass ratio and bulge-to-total mass ratio through the variation of the activity of supernovae feedback with the $\alpha_{\rm outflow}$ parameter, star formation in the discs with $\epsilon_\star$ parameter, and, the gas accretion when $M_{\rm satel.,gas}$ goes to the disc after a minor merger while modifying the value of $F_{\rm mgr}$.As discribed in Table 1, in the set of E-labeled models we have modeled galaxies with $\epsilon_{disk,\star} = 0.01, 0.02, 0.035, 0.05, 0.075$ and 0.1; In the A-labeled models, we selected the four values 1.5, 2.0, 2.5 and 3.0 for the $\alpha_{\rm disk,outflow}$ parameter; We also performed simulations to search wether there is any correlation between the studyed properties and the accretion of gas $M_{\rm satel.,gas}$ in the disc or bulge after a minor merger. As we have a special interest in obtaining disk-type galaxies, for the most of the models in Table 1 we have settled $M_{\rm satel.,gas} \rightarrow$ to the disk. In the D and B-labeled models we set $M_{\rm satel.,gas} \rightarrow$ to the disk and bulge while $F_{\rm mgr}$ is settled to $0.2, 0.3$ and 0.4.

To test wheter the values of the above metioned models are physically reliable, we constructed the Tully-Fischer and Color-Magnitude relations of the mock catalogues. This is decribed in the Appendix.

4.2 Searching LG-type Galaxies

Our investigation of the LG can be divided in two parts. The first is intended to study for the different models in Table 1, the formation of MW and M31-type galaxies; In the second one, we study how peculiar are the LG candidates provided from the CLUES simulations in terms of the similarity of their properties compared to the observed ones.

To study the similarity between the observed and mock galaxies is necessary to make some definitions, first, we call a galaxy as an object globally characterized through a disc stellar mass $M_{\rm disc,\star}$, disc gas mass $M_{\rm disc,gas}$, bulge stellar mass $M_{\rm bulge,\star}$ and $V_{\rm rot}$; Then, to compare observed galaxies and the simulated ones, we pourly define a coordinate space S where a point P has four independ coordinates $P(\delta p_1, \delta p_2, \delta p_3, \delta p_4)$. We define each δp_i as

$$\frac{p_{{\rm obs},i} - p_{{\rm sim},i}}{p_{{\rm obs},i}}, \tag{7}$$

where $p_{{\rm obs},i}$ and $p_{{\rm sim},i}$ are the observed and simulated properties respectively. The properties used to calculate δp_i are the above mentioned four properties to characterize a galaxy. The distance from the origin is given by

$$P = \sqrt{\delta p_1^2 + \delta p_2^2 + \delta p_3^2 + \delta p_4^2}. \tag{8}$$

A point at the origin then corresponds to a perfect match between observation and simulation. For any simulated galaxy

Property	MW	Ref.	M31	Ref.
$M_{disk,\star}[10^{10}M_{\odot}]$	$3.3-4.5$	(1)	$7-10$	(2)
$M_{disk,gas}[10^{10}M_{\odot}]$	$0.6-0.8$	(3)	$0.5-0.6$	(4)
$M_{bulge,\star}[10^{10}M_{\odot}]$	$0.5-1.2$	(3)	$1.9-3.3$	(2)
V_{circ}[Km/s]	238	(5)	275 ± 5	(6)

Table 2. Observational estimations for different properties of the LG, where(1)Zheng et al. (2001),(2) Geehan et al. (2006b), (3)Yin et al. (2009b), (4) Nieten et al. (2006), (5)Battaglia et al. (2005), (6)Seigar et al. (2008).

the lowest the distance the highest the similarity to the observed.

Now, in order find lights about whether there is any set of values of our selected parameters (Section 4.1) that changes the amount of MW and M31-type of galaxies. we accounted the amount of galaxies $N(P)$ similar to the MW and M31 under a ranges of the calculated distances P, studyed its variations as a function of the parameters of interest (Section 4.1).

4.3 Modeling the LG candidates

We proceded to model semi-analyticaly the pairs of LG candidates available from the three WMAP5 boxes of CLUES.

Two experiments were performed. Where we settled the space parameter of the two experiments to a WMAP5 cosmology and $M_{\rm satel.,gas}\rightarrow$ to the disk component of the galaxy.

The first experiment was intended to recreate the experiment of the A-labeled models of Table 1, so, we simulated the LG halo candidates for different values of $\alpha_{\rm disk,outflow}$ ranging from 1.5 to 3.0 in steps of 0.075. For each of the values of $\alpha_{\rm disk,outflow}$, we repeated the simulation over 100 times and calculated the medians of the properties of MW and M31; In the second experiment, we recreate the experiement of the E-labeled models. We simulated the LG candidates through 20 different models of $\epsilon_{\rm disk,\star}$, starting from 0.005 in steps of 0.005 up to 0.1, repeated the simulation 100 times for each value of $\epsilon_{\rm disk,\star}$ and calculated the medians of the properties as well. Finally it was also applied the same searching criteria of equation 8 to look for similarities between the LG modeled pairs and the observed M31 and MW.

5 RESULTS AND DISCUSION

5.1 Baryonic Properties

Besides, as we stated in Section **??**, we developed four experiments intended to study the changes in the stellar-to-dark matter ratio, gas-to-total mass ratio and bulge-to-total mass ratio of the simulated galaxies according to the variation in the different models of $\alpha_{\rm outflow}$, $\epsilon_{\star}$, $F_{\rm mgr}$ and $M_{\rm satel.,gas}\rightarrow$, as described in Table 1.

In Figure 1 are presented the results of three of the above mentioned experiments. The three panels of the left row show the results of the modification of the supernovae activity through four different values of $\alpha_{\rm outflow}$ in the disk component of the simulated galaxies, the A-labeled models of Table 1; The three panels of the central row correspond to the E-labeled models,where we modeled our halo population for six different values of $\epsilon_{\rm disk,\star}$; And, in the three right panels are the results of the D-labeled models, where it is modified the value of the $F_{\rm mgr}$ parameter when $M_{\rm satel.,gas}\rightarrow$ is settled to the disk component.

The panels on top of Figure 1 show the calculated medians of the stellar-to-dark matter ratio relations of each of the experiments, the central panels are the medians of the gas-to-total mass ratio as a funcion of the stellar mass and the ones at the bottom are medians of the bulge-to-total mass ratio as a function of the stellar mass. In the plot at the left on top, galaxies with a total stellar mass content below $3.2\times10^{10}M_{\odot}$ shows a decrease in the amount of the stellar content as it is increased the rate of ejected mass by supernovae, and then, as it is expected, the amount of gas content is increased as can be seen at the left central plot. The morphology of the galaxies is affected as well. Shown at the bottom left panel of Figure 1, the net effect of increasing the $\alpha_{\rm disk,\ outflow}$ parameter produces a decrease of the bulge-to-total mass ratio, so, it increases the amount of disk galaxies. Nevertheless the four values of the $\alpha_{\rm disk,\ outflow}$ parameter keep the the gas-to-total mass ratio relations under good agreement with observations and the bulge-to-total mass ratio relations behaves as it is espected, only the values between 2.5 and 3.0 are the ones thatcan enclose the stellar-to-halo mass relation. 2.5 and 3.0 are respectively upper and lower limits of $\alpha_{\rm disk,\ outflow}$ for the stellar-to-halo mass relation of Moster et al. (2010).

In the top central panel of Figure 1, the stellar-to-halo mass relation show a trend related to the star formation in the disk component of galaxies. As $\epsilon_{\rm disk,\star}$ increases the faint end of the stellar-to-halo mass relation tend to decrease while the bright end increases. It has to be remarked that while the stellar-to-halo mass relation changes, the calculated medians of the relation for the six different models remain almost fixed arround the peak of the relation at $1\times10^{12}M_{\odot}$. In the central panel, a low star formation rate in galaxies with a stellar mass lower than $3.2\times10^{10}M_{\odot}$ increase the gas-to-total mass ratio. In the central bottom panel we can see the increase of the $\epsilon_{\rm disk,\star}$ clearly modifies the morphology of galaxies. A higher $\epsilon_{\rm disk,\star}$ increases the disk component masses of the whole population of simulated galaxies and then the abundace of disk galaxies is increased. Nevertheless the gas-to-total mass ratio relation keeps inside the observations for the different E-labeled models when is compared to the data provided in Bell et al. (2003b) and Bell et al. (2003a), the highest values of $\epsilon_{\rm disk,\star}$ are the ones that provide a relation closer to the one of Moster et al. (2010). The three right panels of Figure 1 show the results of the D-labeled models where it has been settled $M_{\rm satel.,gas}\rightarrow$ to the disk component and simulated for different values of $F_{\rm mgr}$. It was not found any correlation between the $F_{\rm mgr}$ parameter and the calculated properties, not even when $M_{\rm satel.,gas}\rightarrow$ was settled to the bulge in the B-labeled models.

5.2 Abundance of M31 and MW-type galaxies

Now, we will analyse how changes the abundance of LG-type galaxies for the group of experiments defined in Table 1. To do that, we selected halos with a $z=0$ virial mass between $11.5<\log_{10}M_{\rm DM}/M_{\odot}<12.5$; calculated $N(\Delta\varepsilon)$ in ranges

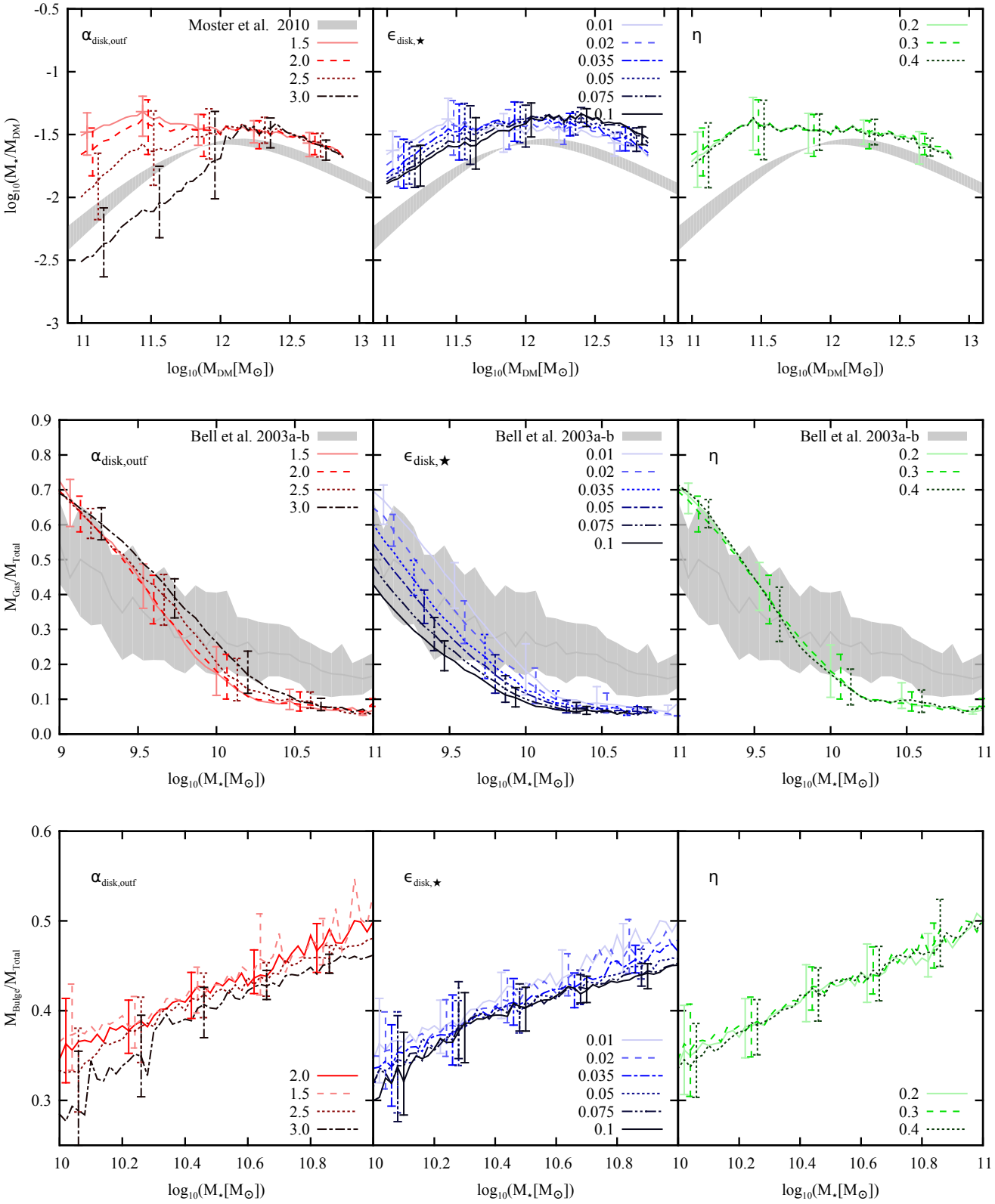

Figure 1. Top: Calculated medians of the stellar-to-halo mass relation compared against the relation of Moster et al. (2010) between the first and thirdth quartils. Central: Medians of the gas-to-total mass fraction as a function of the stellar mass compared to Bell et al. (2003b) and Bell et al. (2003a) between the first and thirdth quartils. Bottom: Medians of the bulge-to-total mass fraction as a function of the stellar mass. The first row of the three plots correspond to the variation of the $\alpha_{\rm outflow}$, the second to the variation of $\epsilon_\star$ and the last to the variation of $F_{\rm mgr}$ when the gas of the satellite goes to the disk of the galaxy. The error bars of each line correspond to the range of the data between the first and third quartils.

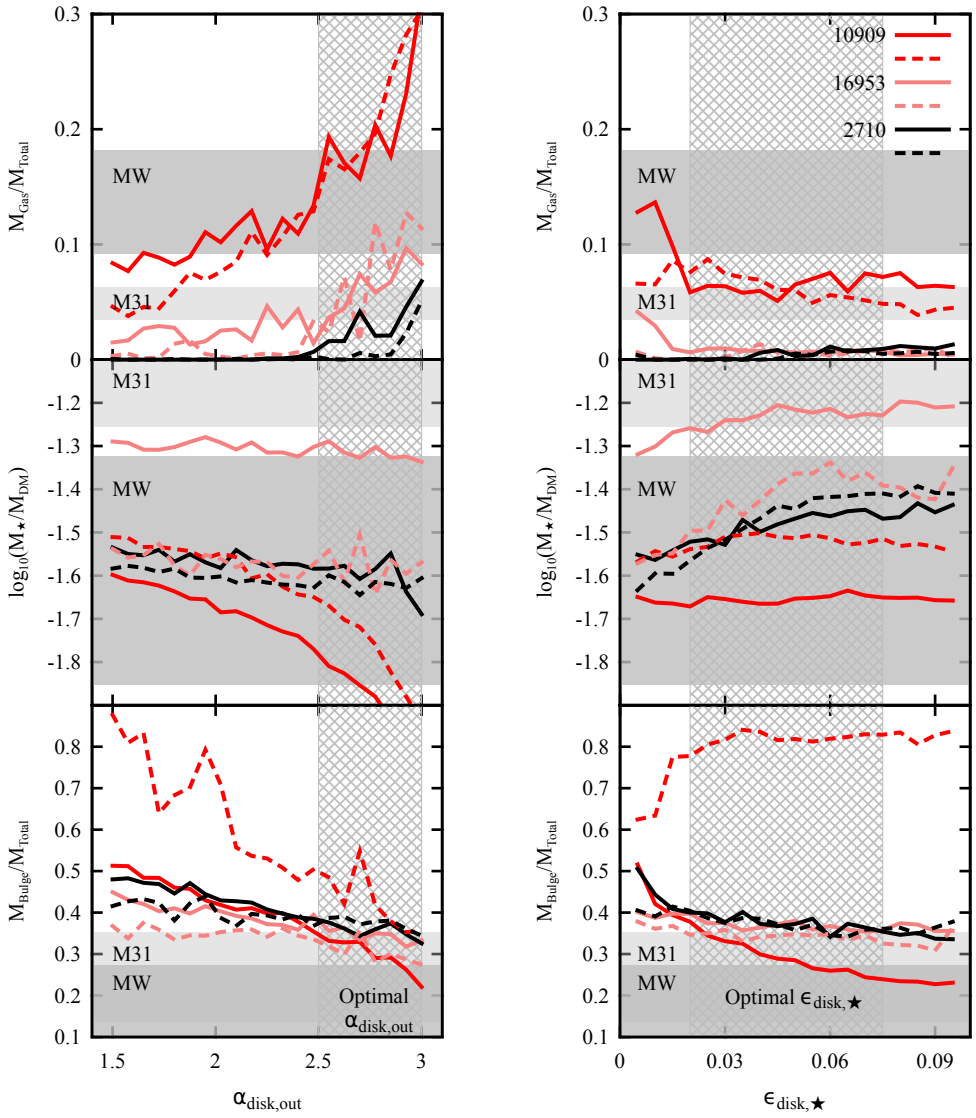

Figure 2. Estimated medians of the modeled properties for the MW and M31 as a function of $\epsilon_\star$ on the right and $\alpha_{\rm outflow}$ on the left. Top: Gas-to-total mass ratio. Central:Stellar mass-to-dark matter mass ratio relation. Bottom: Bulge-to-total mass ratio relation. Horizontal shaded regions correspond to the observational estimations of the MW and M31. The striped regions correspond to the values of the parameters that produce best agreement to the stellar-to-halo mass, gas-to-total mass relations and bulge fraction.

of $\Delta\varepsilon$ for the observed properties of the MW and M31 in Table 2; and, study the $N(\Delta\varepsilon)$ of the lowest values of $\Delta\varepsilon$ as a function of function of $\alpha_{outflow}$, $\epsilon_\star$, $F_{\rm mgr}$ for the different models.

In Figure 3 are plotted the $N(\Delta\varepsilon)$ of the three lowest values of$\Delta\varepsilon$ for MW and M31-type galaxies as a function of $\alpha_{\rm outflow}$ calculated for the set of A-labeled models of Table 1, where the value of $\alpha_{\rm outflow}$ was increased from 1.5 in steps of 0.5 to 3.0. It can be observed that higher values of $\alpha_{\rm outflow}$ increases the amount of LG-type galaxies but priviledges the increase of the abundace of MW-type galaxies more than that of M31-type galaxies.

Nevertheless an increase of the value of $\alpha_{\rm outflow}$ would produce a higher amount of LG-type galaxies, the overstate of the supernovae feedback activity produces a decrease of the stellar-to-halo mass relation for halos with $M_{\rm DM} \leq 1 \times 10^{12} M_\odot$ as can be seen at the plot at the left on top of the Figure 1. We found that under the space parameter configuration of the simulated A-labeled models, the proper values of $\alpha_{\rm outflow}$ for modeling the supernovae feedback through equation 6 can only be between $2.5 \lessapprox \alpha_{\rm outflow} \lessapprox 3.0$, and, to increase the abundance of disk galaxies and then LG-type galaxies, should be choosen the highest values $\alpha_{\rm outflow}$ below 3.0.

We also made an analysis like the above with the $\epsilon_\star$ parameter for the E-labeled models. Figure 4 shows the values of $N(\Delta\varepsilon)$ for the three lowest values of $\Delta\varepsilon$ calculated for LG-type galaxies as a function of $\epsilon_\star$.

Even though higher values of $\epsilon_\star$ increases the abundace of disk galaxies, the increase of the star formation in the disk component of the sample of simulated galaxies does not

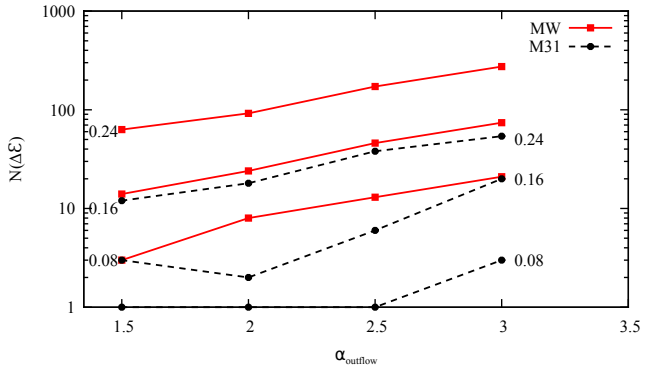

Figure 3. $N(\Delta\varepsilon)$ as a function of $\alpha_{\rm outflow}$. $N(\Delta\varepsilon)$ for the three lowest values of $\Delta\varepsilon = 0.08, 0.16, 0.24$ as a consecuense of the variation of $\alpha_{\rm outflow}$ parameter.

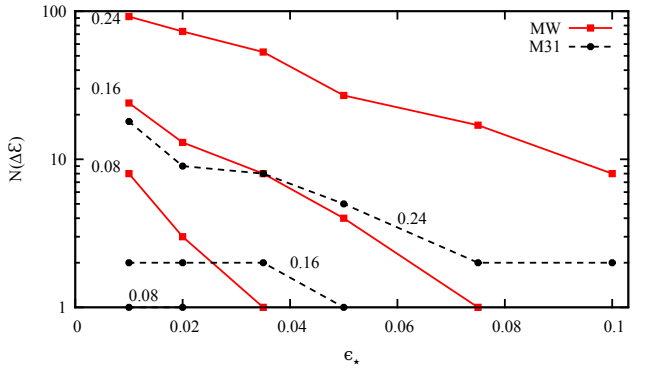

Figure 4. $N(\Delta\varepsilon)$ as a function of $\epsilon_\star$. $N(\Delta\varepsilon)$ for the three lowest values of $\Delta\varepsilon = 0.08, 0.16, 0.24$ as a consecuenseof the variation of $\epsilon_\star$ parameter.

favorate the formation of LG-type galaxies, on the contrary, the decrease of the parameter favorates it.

The performed D-labeled simulations with different values of $F_{\rm mgr}$; intended to see wether this parameter affects the formation or LG-type galaxies or not,showed no correlation between $F_{\rm mgr}$ and $N(\Delta\varepsilon)$. As can be seen at the right plots of Figure 1, the shape of the simulated properties for our sample galaxies is not affected by the $F_{\rm mgr}$ parameter. Nevertheless of the previous result, we found that the redirection of the gas of a satellite after a minor merger to the disk instead of the bulge does favorate the searched situation, as it can be seen in Figure 5 where we compare $N(\Delta\varepsilon)$ of models R2 and R3 calculated for MW and M31-like galaxies.

5.3 The MW and M31 candidates

As described in section , to study the LG candidates of the CLUES WMAP5 simulations we runned 20 models where we repeated over 100 times the estimation the properties in each of the models and the calculated the medians of each property. In Figure 2 can be observed the estimated medians for the stellar mass, gas fraction and bulge fraction as a function of the parameters $\epsilon_\star$ and $\alpha_{\rm outflow}$. It can be observed that each pair of LG corresponding to the same simulations

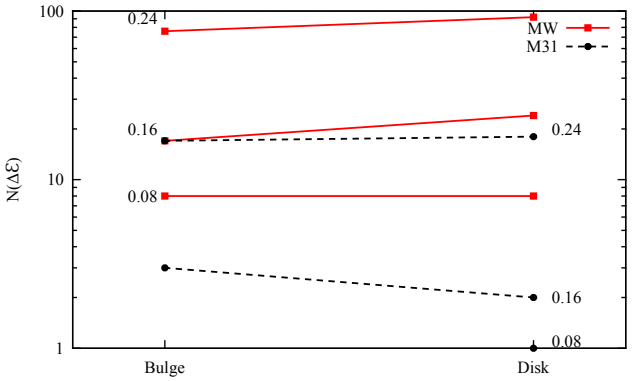

Figure 5. The values of $N(\Delta\varepsilon)$ for the three lowest values of $\Delta\varepsilon = 0.08, 0.16, 0.24$ when the gas of a satellite after a merger goes to the disk and to de bulge.

have a similar behavior as the values of the parameters are changed.

6 CONCLUSIONS

ACKNOWLEDGMENTS

REFERENCES

Abazajian K. N., Adelman-McCarthy J. K., Agüeros M. A., Allam S. S., Allende Prieto C., An D., Anderson K. S. J., Anderson S. F., Annis J., Bahcall N. A., et al. 2009, ApJS, 182, 543

Battaglia G., Helmi A., Morrison H., Harding P., Olszewski E. W., Mateo M., Freeman K. C., Norris J., Shectman S. A., 2005, MNRAS, 364, 433

Baugh C. M., Lacey C. G., Frenk C. S., Granato G. L., Silva L., Bressan A., Benson A. J., Cole S., 2005, MNRAS, 356, 1191

Bell E. F., McIntosh D. H., Katz N., Weinberg M. D., 2003a, ApJL, 585, L117

Bell E. F., McIntosh D. H., Katz N., Weinberg M. D., 2003b, ApJS, 149, 289

Benson A. J., 2010, ArXiv e-prints

Benson A. J., Bower R., 2010, MNRAS, 405, 1573

Bett P., Eke V., Frenk C. S., Jenkins A., Helly J., Navarro J., 2007, MNRAS, 376, 215

Boissier S., Prantzos N., 1999, MNRAS, 307, 857

Braun R., Walterbos R. A. M., 1992, ApJ, 386, 120

Capaccioli M., Schipani P., 2011, The Messenger, 146, 2

Cram T. R., Roberts M. S., Whitehurst R. N., 1980, A&AS, 40, 215

Croton D. J., Springel V., White S. D. M., De Lucia G., Frenk C. S., Gao L., Jenkins A., Kauffmann G., Navarro J. F., Yoshida N., 2006, MNRAS, 365, 11

Dame T. M., 1993, in Holt S. S., Verter F., eds, Back to the Galaxy Vol. 278 of American Institute of Physics Conference Series, The distribution of neutral gas in the Milky Way. pp 267–278

Dehnen W., Binney J., 1998, MNRAS, 294, 429

Forero-Romero J. E., Hoffman Y., Yepes G., Gottlöber S., Piontek R., Klypin A., Steinmetz M., 2011, ArXiv e-prints

Geehan J. J., Fardal M. A., Babul A., Guhathakurta P., 2006a, MNRAS, 366, 996

Geehan J. J., Fardal M. A., Babul A., Guhathakurta P., 2006b, MNRAS, 366, 996
Gottloeber S., Hoffman Y., Yepes G., 2010, ArXiv e-prints
Hoffman Y., Ribak E., 1991, ApJL, 380, L5
Karachentsev I. D., Karachentseva V. E., Huchtmeier W. K., Makarov D. I., 2004, AJ, 127, 2031
Keller S. C., Schmidt B. P., Bessell M. S., Conroy P. G., Francis P., Granlund A., Kowald E., Oates A. P., Martin-Jones T., Preston T., Tisserand P., Vaccarella A., Waterson M. F., 2007, PASA, 24, 1
Klypin A., Zhao H., Somerville R. S., 2002, ApJ, 573, 597
Klypin A. A., Trujillo-Gomez S., Primack J., 2011, ApJ, 740, 102
Komatsu E., Dunkley J., Nolta M. R., Bennett C. L., Gold B., Hinshaw G., Jarosik N., Larson D., Limon M., Page L., Spergel D. N., Halpern M., Hill R. S., Kogut A., Meyer S. S., Tucker G. S., Weiland J. L., Wollack E., Wright E. L., 2009, ApJS, 180, 330
Kulkarni S. R., Heiles C., 1987, in Hollenbach D. J., Thronson Jr. H. A., eds, Interstellar Processes Vol. 134 of Astrophysics and Space Science Library, The atomic component. pp 87–122
LSST Science Collaboration Abell P. A., Allison J., Anderson S. F., Andrew J. R., Angel J. R. P., Armus L., Arnett D., Asztalos S. J., Axelrod T. S., et al. 2009, ArXiv e-prints
Moster B. P., Somerville R. S., Maulbetsch C., van den Bosch F. C., Macciò A. V., Naab T., Oser L., 2010, ApJ, 710, 903
Muñoz-Cuartas J. C., Macciò A. V., Gottlöber S., Dutton A. A., 2011, MNRAS, 411, 584
Muñoz-Cuartas J. C., Müller V., 2012, MNRAS, 423, 1583
Newberg H. J., China L. p. o., in LAMOST P., (PLUS) U., 2009, in American Astronomical Society Meeting Abstracts #213 Vol. 41 of Bulletin of the American Astronomical Society, The LAMOST Spectroscopic Survey of Milky Way Stars (LEGUE). p. 416.14
Nieten C., Neininger N., Guélin M., Ungerechts H., Lucas R., Berkhuijsen E. M., Beck R., Wielebinski R., 2006, A&A, 453, 459
Pizagno J., Prada F., Weinberg D. H., Rix H.-W., Pogge R. W., Grebel E. K., Harbeck D., Blanton M., Brinkmann J., Gunn J. E., 2007, AJ, 134, 945
Press W. H., Schechter P., 1974, ApJ, 187, 425
Seigar M. S., Barth A. J., Bullock J. S., 2008, MNRAS, 389, 1911
Springel V., 2005, MNRAS, 364, 1105
Springel V., 2010, MNRAS, 401, 791
Springel V., Wang J., Vogelsberger M., Ludlow A., Jenkins A., Helmi A., Navarro J. F., Frenk C. S., White S. D. M., 2008, MNRAS, 391, 1685
Springel V., White S. D. M., Jenkins A., Frenk C. S., Yoshida N., Gao L., Navarro J., Thacker R., Croton D., Helly J., Peacock J. A., Cole S., Thomas P., Couchman H., Evrard A., Colberg J., Pearce F., 2005, Nature, 435, 629
Teyssier R., 2002, A&A, 385, 337
Tonry J. L., Dressler A., Blakeslee J. P., Ajhar E. A., Fletcher A. B., Luppino G. A., Metzger M. R., Moore C. B., 2001, ApJ, 546, 681
Tumlinson J., 2006, ApJ, 641, 1
White S. D. M., Frenk C. S., 1991, ApJ, 379, 52

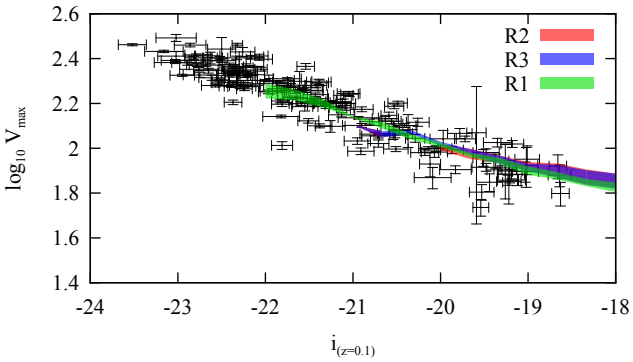

Figure 6. Tully fischer relation. The magnitudes where calculated without dust extintion and the parameters of the models can be seen at Table 1 as R1, R2 and R3. The error bars correspond to the results of Pizagno et al. (2007).

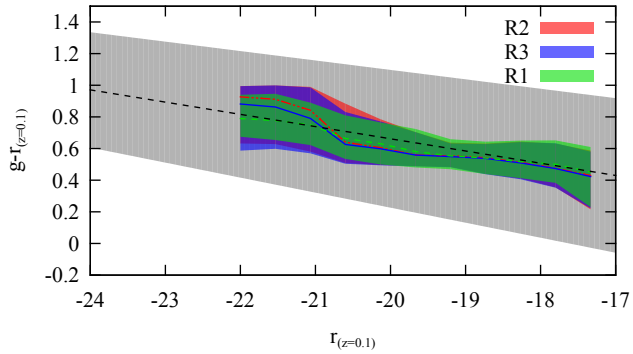

Figure 7. Color magnitud relation. Magnitudes were calculated without extintion. This is the reference simulation presented in table 1 as R1, R2 and R3. The shaded region correspond to a scatter of 2σ from the work of Muñoz-Cuartas & Müller (2012).

White S. D. M., Rees M. J., 1978, MNRAS, 183, 341
Widrow L. M., Dubinski J., 2005, ApJ, 631, 838
Willick J. A., Courteau S., Faber S. M., Burstein D., Dekel A., Strauss M. A., 1997, ApJS, 109, 333
Yin J., Hou J. L., Prantzos N., Boissier S., Chang R. X., Shen S. Y., Zhang B., 2009a, A&A, 505, 497
Yin J., Hou J. L., Prantzos N., Boissier S., Chang R. X., Shen S. Y., Zhang B., 2009b, A&A, 505, 497
Zheng Z., Flynn C., Gould A., Bahcall J. N., Salim S., 2001, ApJ, 555, 393

7 APPENDIX: TESTING THE RESULTS FROM GALACTICUS

To build the Tully-Fischer relation we used the maximum velocity of the disc component of the discs galaxies ($M_{\rm Bulge}/M_{\rm Total} \leq 0.3$).

We calculated the Tully-Fisher and Color-Magnitude relations for each of the models in Table 1. To build the Tully-Fisher relation, we proceded selecting the maximum velocity between the bulge and disk components of disk

galaxies, and defined disks as galaxies with a bulge-to-total mass ratio $M_{\rm bulge}/M_{\rm tot} \leq 0.3$.

In Figure 6 are shown de scatters of the maximum velocity between the first and thirth quartils as a function of magnitude in the i-band without dust extintion of the data of the three benchmarks R1, R2 and R3 compared to the data of the SDSS (Pizagno et al. 2007). It can be seen the resulting Tully-Fisher relations of each of the benchmarks reproduce accurately the one of the SDSS. In general none of the calculated Tully-Fisher relations of any of the simulated models deviate significantly from ones shown in 6. We have also calculated the Color-Magnitude diagrams without dust extintion of the three mentioned benchmarks. In Figure 7, the scatter of the color between the first and thirth quartils and the medians as a function of the r-band reproduce accurately the estimated Color-Magnitude relation of the SDSS (Muñoz-Cuartas & Müller 2012). Again, in general, all the other simulated models of the calculated medians does not deviate significantly from the estimations of the best fit of the mean of the SDSS and remains inside of the 3σ estimated deviation of the Color-Magnitude relation.